Spatial, Temporal and Environmental Effects on LoRa Link Characteristics: Evidence from a Sustainable Sensor Network in London

Dongyi Ma*
The Bartlett Centre for Advanced Spatial Analysis
University College London
London, United Kingdom
dongyi.ma.21@ucl.ac.uk

Huanfa Chen
The Bartlett Centre for Advanced Spatial Analysis
University College London
London, United Kingdom
huanfa.chen@ucl.ac.uk

Martin De Jode
The Bartlett Centre for Advanced Spatial Analysis
University College London
London, United Kingdom
m.dejode@ucl.ac.uk

Andrew Hudson-Smith
The Bartlett Centre for Advanced Spatial Analysis
University College London
London, United Kingdom
a.hudson-smith@ucl.ac.uk

Mo Sha
Knight Foundation School of Computing and Information Sciences
Florida International University
Miami, United States
msha@fiu.edu

***Abstract*— LoRa/LoRaWAN has been increasingly adopted in urban outdoor sensor networks, yet its long-term communication performance in complex urban environments remains under-documented. This paper presents a one-year empirical evaluation of LoRaWAN link performance using 15 solar-powered sensors deployed in London, examining how distance, land cover, air temperature, humidity, season, and time of day affect received signal strength indicator (RSSI), signal-to-noise ratio (SNR), spreading factor (SF) under Adaptive Data Rate (ADR), and packet loss rate (PLR). Results show that transmission distance is the dominant factor of RSSI and SNR variations, while land cover and diurnal variation in the local environment also contributed to site-specific differences in link quality. Temperature, humidity, and season show weak or negligible associations. Higher ADR-assigned SF values are generally observed under weaker links, although elevated PLR at one site indicates the need for improved SF selection algorithms in complex urban conditions. Overall low PLR confirms the effectiveness of LoRa/LoRaWAN system for urban environmental data collection, with findings provide field evidence to inform the design of future urban sensing systems.**

Keywords—LoRa, Internet of Things, Wireless Sensor Network, Link Characteristics, Adaptive Data Rate

I. INTRODUCTION

LoRa (Long Range) is a physical layer technology that enables long-range, low-power communication in unlicensed sub-GHz bands, while LoRaWAN (Long Range Wide Area Network) defines the communication protocol and network architecture through which battery-powered end devices exchange data with gateways, network servers, and application servers across a wide-area network, typically employing a star-of-stars topology (end devices communicate directly with gateways, and gateways forward received packets to a central network server) optimized for low-power sensing [1]. Due to their characteristics in low power demand, wide coverage, and suitability for battery-powered sensing systems, LoRa and LoRaWAN have been increasingly used in various Internet of Things (IoT) applications, such as environmental monitoring and smart cities, especially for large-scale sensor networks over long term [2]. The LoRa Alliance reports that LoRaWAN devices, networks, and gateways have been deployed across the globe and in numerous industries at scale in multiple national contexts, for example, 70,000 smart streetlights in Uruguay, 150,000 smart water meters in the United Kingdom, 47,000 indoor air-quality sensors in Canada, and public network coverage across more than 1,600 square miles in the United States etc. [3].

Despite these widespread applications, the performance of LoRa/LoRaWAN as claimed by Semtech (10-15km communication range, several years of battery life) is often challenged in outdoor deployments, especially in dense and complex urban environments. A growing body of literature has reported the much less signal propagation distance under non-line-of-sight conditions, varying from 140m to a few kilometers depending on the hardware used, transmission settings and local urban morphology [4], [5], [6]. Recent studies [7], [8] also examined environmental influences on LoRaWAN's performance including spreading factor (SF), signal-to-noise ratio (SNR), received signal power and packet reception behavior. Existing evidence [9], [10], [11] also suggests that weather variations (air temperature and humidity) can affect link stability on SNR, received signal strength indicator (RSSI), and packet reception. However, relatively limited evidence in the field has supported a relationship between the factors and the performance, as much of the existing work has focused on simulation-based evaluation and algorithmic optimization, controlled laboratory experiments, or relatively short-term real-world studies, while comparatively fewer studies have examined these relationships systematically in long-term outdoor deployments.

This study uses a one-year outdoor dataset from 15 identical solar-powered sensors in a microclimate sensor network deployed in London [12], which offers several benefits for examining LoRaWAN performance in a low-obstruction urban park environment. First, the network provides high-resolution (5-minute interval) temperature/humidity observations across a 2 km² urban park with diverse land-cover types (river, trees, grass, concrete, and buildings) and high measurement accuracy (validated against a semiprofessional weather station) supported by improved solar radiation shielding. Second, the network consists of 15 identical bespoke solar-powered sensors based on the Arduino MKR1310, consistently deployed at 2.5 m above ground level, which reduces variation from hardware heterogeneity or installation inconsistency across sites. Third, the network operated continuously for one-year (with data completeness over 99.9%) under default Adaptive Data Rate (ADR) settings, without manual maintenance, battery replacement, or parameter adjustment, thereby providing naturalistic real-world operating condition observations. These characteristics enable an analysis of how distance to the gateway, temperature, humidity, season, time of day, and land-cover type (as explanatory variables) are associated with variations in RSSI, SNR, SF, and packet loss (as response variables) in a long-term outdoor LoRaWAN sensor network.

II. Data and Method

A. The Sensor Network and Study Area

The sensor design and validation are documented in previous publication [13]. All 15 sensors (denoted as P1-P15) communicate with a single gateway (MultiTech Conduit IP67) at 50 m elevation, under LoRaWAN Specification 1.0.2 (125kHz Bandwidth) through Over the Air Activation (OTAA), supported by The Things Network (TTN), a community based LoRaWAN infrastructure. Sensor-to-gateway distances range from 126 m to 1329 m. Originally designed for microclimate monitoring, this network spans across Queen Elizabeth Olympic Park on various land cover types, as shown in Figure 1. Panoramic photo of each deployment site can be found in Appendix A. It's also worth highlighting that these sensors can be broadly grouped into three categories based on their local environment:

(1) P1, P3 and P11 are mounted under deciduous trees, with distance to gateway of 227 m, 185 m, and 1329 m, respectively.
(2) P2, P4 and P8 are located immediately adjacent to the river, with distance to gateway of 143 m, 126 m and 467 m respectively.
(3) The remaining sensors are located mainly on paved surfaces and/or near vegetation or within a few metres to water body, with broadly similar sky view factors (SVF). Among them, P7 is near a stadium entrance and P10 is near a primary school playground which suggests that, in addition to normal traffic activity, these two sites may also be influenced by higher levels of human activity.

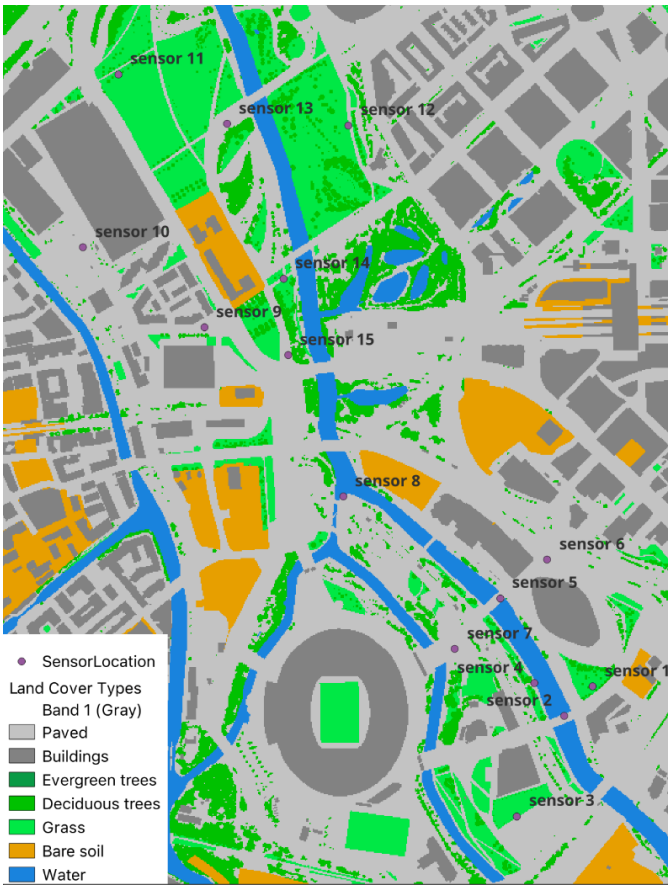

Fig.1. Deployment locations of the 15 bespoke LoRaWAN sensors in Queen Elizabeth Olympic Park, London. Colors indicate seven land-cover types, including paved surfaces, buildings, evergreen trees, deciduous trees, grass, bare soil, and water, derived from OpenStreetMap data and field observations.

B. Data

The sensor network operated continuously without any maintenance since 1st August 2024. To aid seasonal analysis, this study adopts the data obtained until 1st August 2025 as a preliminary examination. Throughout this one-year period, each sensor was programmed to transmit air temperature and humidity data at 5-minute intervals using a fixed payload size and format. In total, more than 1.5 million packets were received during the study period. For each uplink packet received by the gateway and forwarded via TTN, the associated LoRaWAN communication metadata were recorded as follows:

- Frame counter (FCnt, denoted as C_i for the i-th sequential packet): a sequential numerical identifier which increments by one for each packet transmitted by a sensor.
- Received signal strength indicator (RSSI): a measure (in dBm) of the received signal strength of each packet at the gateway.
- Signal-to-noise ratio (SNR): a measure (in dB) of the ratio of packet signal power to background radio noise.
- Spreading Factor (SF): a tuneable modulation parameter (unitless, ranging from 7 to 12 in our case) that determines the speed and range of the LoRa signal.

- Timestamp: the precise time at which the packet was received by the gateway.
- Gateway identifier: to document the receiving gateway.

C. Packet Loss and Packet Loss Rate Calculation

In this study, packet loss is defined as a scenario where a sensor successfully transmits a data packet (and thus incremented its frame counter) but the packet is not received by the gateway or forwarded to the application server due to network issues. It was only assessed when the devices were known to be operational. Any period during which a device failed to transmit for more than 24 consecutive hours was also excluded, as this was assumed to correspond to either a power interruption or gateway/service downtime rather than normal packet loss. In our case, packet loss exists as short transmission gaps (e.g., expecting a message every 5 minutes, but sometimes receiving the next message 10 or 30 minutes or even hours). As gateway-side raw logs were not available for this study, lost transmissions were inferred using the received FCnt sequence. Packet loss rate (PLR) is defined as the proportion of data packets sent by the device that fail to reach any gateway.

Let C_i denote the frame counter of the i-th received packet, and C_{i-1} denote the frame counter of the packet immediately preceding it. The difference between them is expressed as:

$$\Delta C_i = C_i - C_{i-1} \tag{1}$$

If $\Delta C_i = 1$, transmission was continuous, and no packet was lost. If $\Delta C_i > 1$, the number of packets lost between these two receptions equals the size of the gap minus one. The number of packets lost for each interval is therefore calculated as:

$$N_{loss,i} = \begin{cases} (\Delta C_i - 1); & \text{if } \Delta C_i > 1 \\ 0; & \text{if } \Delta C_i = 1 \\ \text{undefined}; & \text{if } \Delta C_i \leq 0 \end{cases} \tag{2}$$

where $N_{loss,i}$ denotes the number of packets lost between two consecutive received packets. When $\Delta C_i \leq 0$, it indicates that the device has rebooted or rejoined the network, causing FCnt to reset to zero. In such cases, packet loss cannot be determined because the duration of the disconnection is unknown. These intervals are therefore excluded from the analysis. Similarly, when both $C_{i-1}=0$ and $C_i=0$, the reliability of the link during that period is unknown and excluded. After calculating $N_{loss,i}$ for all valid intervals, the total number of lost packets for each sensor is obtained by summing across all intervals:

$$N_{loss} = \Sigma N_{loss,i} \tag{3}$$

The number of successfully received packets ($N_{received}$) is the count of all packets logged by TTN during the operational period, excluding those removed in preprocessing. The total expected number of packets equals the sum of lost and received packets. Thus PLR is calculated as:

$$PLR = \frac{N_{loss}}{N_{loss} + N_{received}} \tag{4}$$

III. Results

A. Distance-Related Variation in RSSI, SNR, PLR and SF under ADR Operation

A maximum sensor-to-gateway distance of 1329 m was observed under the relatively open park conditions and the farthest nodes appeared to operate under conditions close to the LoRa receiver demodulation limit. As shown in Figure 2, in general, both RSSI and SNR tend to decrease with distance. RSSI declined from approximately –77 dBm at 126 m to around –116 dBm at distances beyond 1 km, with a strong negative correlation with distance (Pearson correlation $r \approx -0.95$). SNR showed a similar pattern, decreasing from 7–8 dB for sensors within 300 m to negative values (–2 to –7 dB) for sensors beyond 900 m. This suggests a transition from relatively stable to weaker link conditions with increasing distance, although the lowest RSSI and SNR site (P10) did not occur at the greatest distance, indicating that while distance was the dominant factor, local obstructions or site-specific environmental conditions may also have influenced actual link performance.

Poorer RSSI and SNR did not necessarily correspond to higher packet loss across the network. Under ADR operation, sensors with lower RSSI and SNR were assigned higher SF values and sensors beyond about 800 m more frequently operated at SF9–SF10. P10 located 1113 m from the gateway showed the lowest RSSI and SNR and together with highest average SF, but its PLR was less than half of P12 with a slightly shorter distance at 1099 m, which suggests that ADR may have helped maintain packet delivery under worse link conditions. However, P12 exhibited nearly twice the PLR of all the other sites despite not having the lowest RSSI or SNR, suggesting that the current TTN ADR strategy, which primarily adjusts SF on the basis of SNR margin may not fully account for local LoRa communication conditions in complex urban environments, and suggests the critical need to develop new SF selection algorithms (potentially adapts SF at runtime based on measured network performance on PLR). At the same time, elevated PLR at P12 may also reflect local obstruction or other site-specific conditions that were not captured by distance alone.

No clear evidence was found that communication quality was systematically associated with local land-cover conditions, as sensors installed under trees or adjacent to water did not consistently show poorer link performance. Across the network, sensors in the northern half of the park tended to show poorer link quality than those in the southern half, where most distances were within 500 m.

Figure 3 provides a spatial interpretation map of link quality across QEOP. The RSSI map presents a clear spatial gradient, with higher values in the south near the gateway and progressively lower values toward the northern boundary, which is consistent with the trend shown in Figure 2 and suggests that distance was the main control on RSSI across the deployment. The SNR map shows a similar decline away from the gateway but with greater local variation. For example, P5 showed lower SNR than the more distinct P6, indicating that distance did not fully explain the spatial variation in SNR where local site conditions, surrounding building heights and human activity interferences may also contribute to the differences.

Fig.2. Observed relationship betwwen distance and network performance.

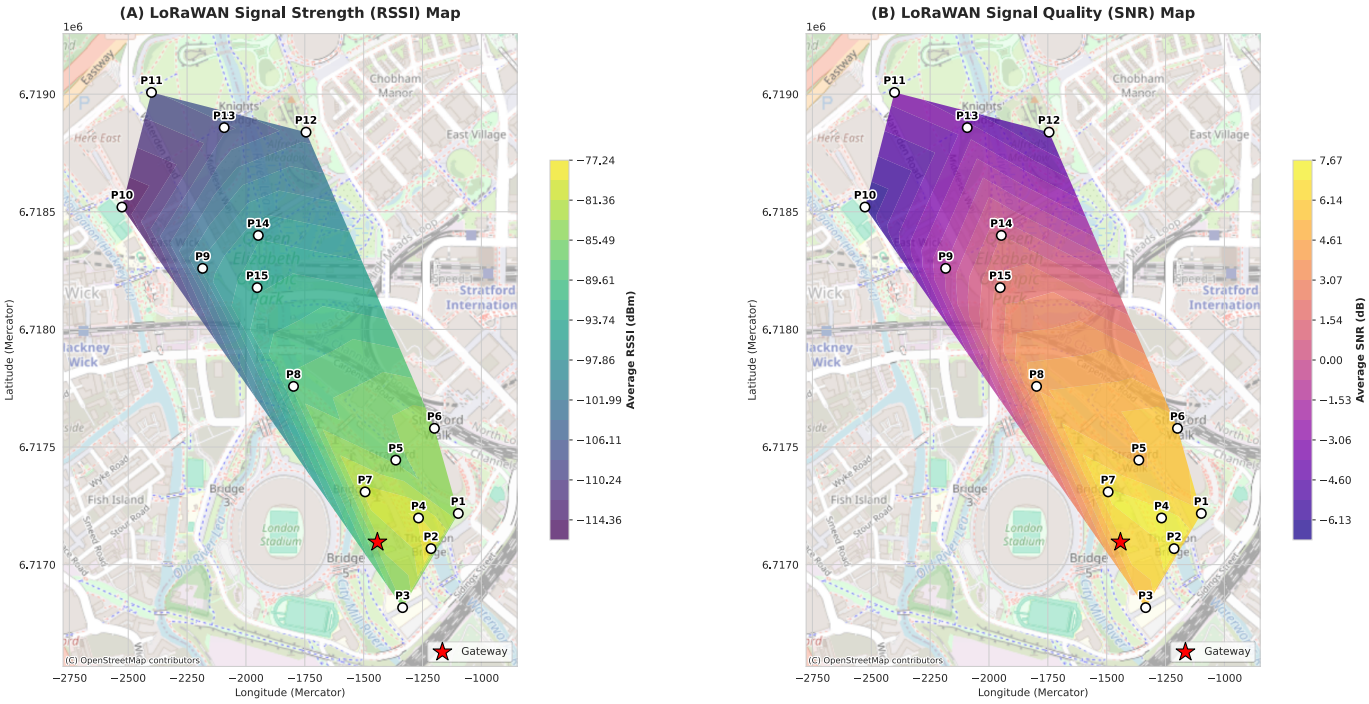

Fig.3. Spatial interpolation of signal quality across QEOP: (A) average RSSI map; (B) average SNR map.

B. *Temperature and Humidity Associations with RSSI/SNR*

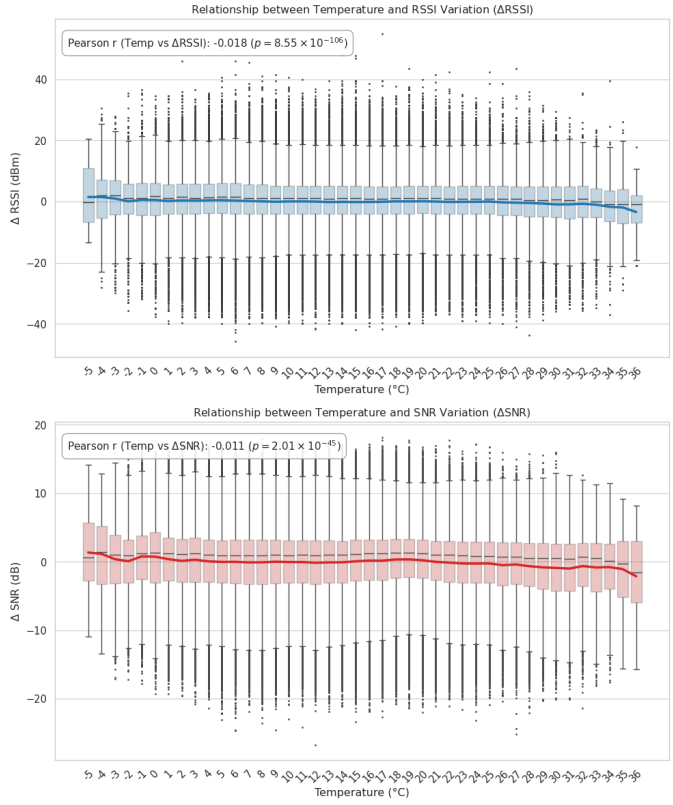

Fig.4. Observed relationship betwwen temperature and SNR/RSSI variation.

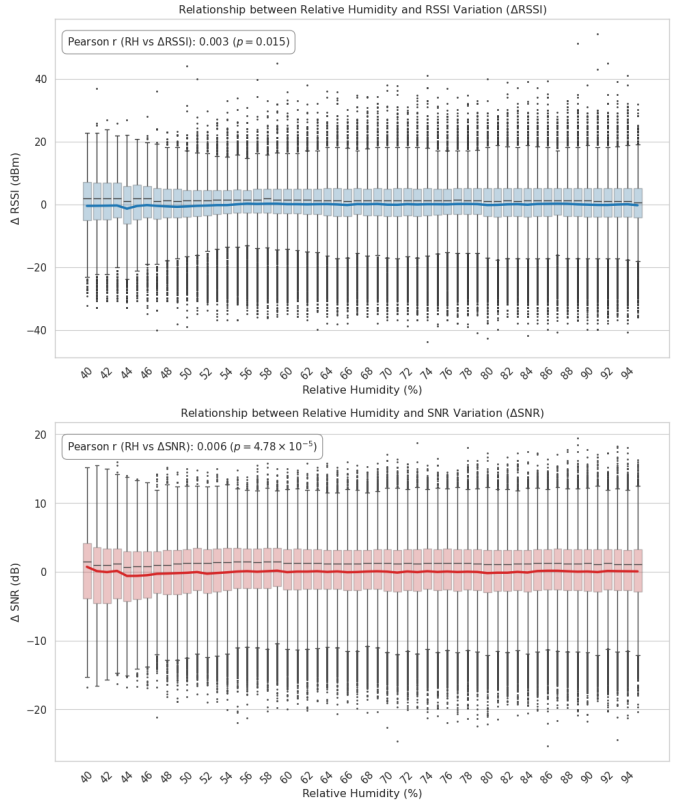

Fig.5. Observed relationship between humidity and SNR/RSSI variation.

Figures 4 and 5 demonstrate how air temperature and relative humidity (RH) were associated with variation in RSSI and SNR. Temperature and RH were measured using the HDC1080 sensor chip (typical accuracy: ±0.2 °C for temperature and ±2% RH according to the manufacturer's datasheet), and RH records equal to 99.99% were excluded as outliers during preprocessing. ΔRSSI and ΔSNR are calculated as deviations from each sensor's baseline mean value to reduce spatial confounding from inherent differences among sites (sensor-to-gateway distance, local urban morphology, and inter sensor bias). Under ADR operation, SF is adjusted by the network in response to link conditions, while PLR reflects a downstream outcome influenced by multiple factors, thus these indirect indicators of network performance are not studied in this case.

Over the year, observed air temperature ranged approximately from -5 °C to 36 °C. Across almost all temperature bins, both ΔRSSI and ΔSNR exhibited wide distributions, while their medians and trend lines remained close to zero, indicating substantial signal variability under similar thermal conditions and suggesting that temperature was only weakly associated with signal variation and produced only small average shifts, although very high temperatures (>35 °C) were associated with lower ΔRSSI and ΔSNR. Similarly, no clear pattern was observed between RH and either ΔRSSI or ΔSNR within the valid non-saturated dataset, suggesting limited explanatory value of the observed signal variation.

C. *Temporal Variations in ΔSNR, ΔRSSI, and PLR*

Figures 6 and 7 present the monthly and diurnal averages of ΔRSSI, ΔSNR, and PLR across the year, each computed as the average across all 15 sensors. Monthly ΔRSSI and ΔSNR remained broadly stable, varying within approximately ±3 dBm and ±2 dB respectively, showing no clear seasonal pattern. P9 and P15 exhibited the largest month-to-month fluctuations, which may reflect site-specific influences associated with their roadside intersection and road construction site settings, as LoRa links in built-up environments can be sensitive to dynamic propagation changes caused by metal objects and moving vehicles [14]. A similarly stable pattern was observed at the diurnal scale, however, P10 exhibited the strongest within-day variation in both ΔRSSI and ΔSNR with poorer link quality at daytime, possibly due to the immediate proximity of a primary school playground, where local activity may have introduced stronger short-term local disturbance. P10 also showed the largest diurnal variations in received packets, especially around midday, with hourly counts decreasing from 4318 at the nocturnal maximum to 4014 at noon (approximately 7.0%). Similarly, diurnal PLR also showed slightly higher values during daytime than at night across several sites, potentially due to the lower RSSI and SNR associated with daytime. Nevertheless, network-wide PLR remained low overall, with an average of 0.01%, with monthly values consistently below 0.15% for nearly all months except for February 2025 (0.23%), indicating that the system sustained high data completeness and near-continuous data transmission without clear degradation over time or seasonal changes due to the reduced energy for the solar-charging system throughout winter in a mid-latitude city, although observations are ongoing to evaluate its long-term sustainability.

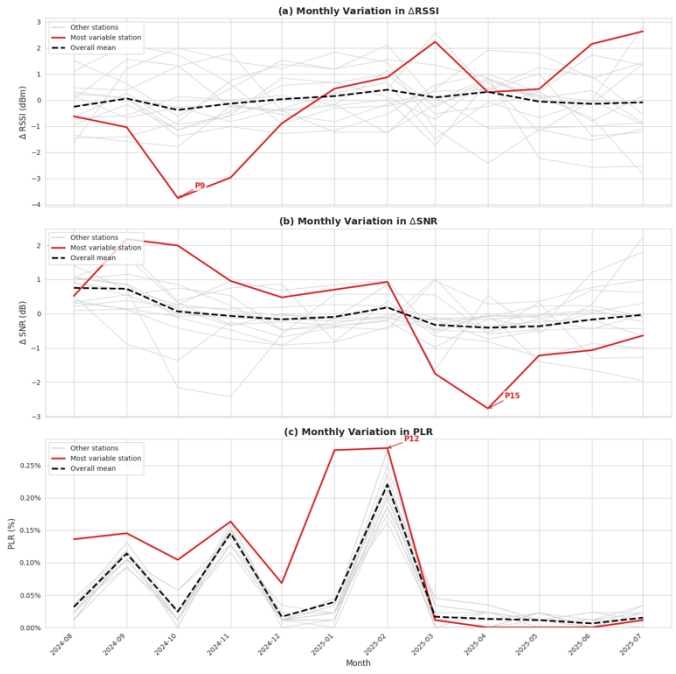

Fig.6. Average monthly variations in ΔRSSI, ΔSNR and PLR.

Fig.7. Average diurnal variations in ΔRSSI, ΔSNR and PLR.

IV. Discussion

In this study, the sensor network reached a maximum sensor-to-gateway distance of 1329 m under relatively open park conditions, which is broadly consistent with previous studies of LoRa communication range in urban areas and provides a practical reference for expected connection range in similar low-obstruction urban settings. The spatial, temporal and environmental analysis indicate that distance was the main control on LoRa link quality in this deployment, particularly for RSSI, while local environmental context appeared more clearly in SNR. Temperature and humidity showed only weak relationship with link variation, while no clear network-wide seasonal pattern was observed. PLR appeared to peak at 07:00 and 17:00, roughly coinciding with rush-hour periods. Although daytime SNR was generally lower than nighttime values, this pattern was not clearly reflected in SNR, suggesting that SNR on its own may not be the best measure of link reliability in this deployment. Meanwhile, packet loss remained low across the deployment, which suggests that ADR and the physical openness of the site helped maintain packet delivery even where RSSI and SNR declined with distance. However, the persistently higher loss at P12 suggests that TTN ADR strategy could be improved by assigning SF based on PLR. Besides, the panoramic photo dataset may also support future image-based analysis to derive comparable environmental descriptors around each sensor to more localized ADR optimization.

However, the increased signal attenuation for under-canopy near-ground nodes reported by [6] was not clearly observed in this study, indicating that land-cover effects on LoRa links may be conditional on distance, local openness, surrounding obstructions, and weather conditions. In this respect, the present results point to the need for quantitative land-cover characterization in future work: defining multi-scale buffer zones around each sensor to examine how land-cover combinations (vegetation, pavement, buildings, water) influence link performance. Metrics such as SVF, vegetation fraction, building proximity/material may help clarify how local openness and obstruction shape radio performance. These patterns are relevant to future scaling of LoRa-based sensor networks, where connection range, RSSI decline, and SNR variability will shape gateway siting and expected network coverage.

Several limitations should also be noted. First, RH data was not validated against any reference weather station and not calibrated after deployment. 60.76% RH records were excluded since they reached 99.99%, possibly due to condensation on the sensor (which occurs overnight and early morning in the cooler months) or rainfall exposure associated with the open Stevenson screen, which may have introduced additional uncertainty into the RH data, thus the absence of a clear humidity effect may reflect both the physical LoRa signal behavior and data quality limitations. Meanwhile, a larger and more dense deployment where explanatory variables have larger variations, combined with improved sensor protection and additional RH validation, would help to clarify whether temperature/humidity has a systematic role under outdoor conditions. Second, this analysis was strictly constrained to the primary gateway (rx_metadata_0). Any packets that were not successfully demodulated by this gateway, even if they were received by secondary community gateways, were excluded from the signal-quality analysis. This decision was necessary to maintain a fixed spatial baseline, as RSSI and SNR are highly sensitive to path length, local multipath effects, gateway hardware, and surrounding interference conditions, incorporating multiple receiving gateways would have introduced additional confounding and made it more difficult to isolate the influence of temporal and environmental variation. By restricting the dataset to the primary receiving gateway, the analysis could more directly examine how air temperature, humidity, and

diurnal or seasonal variation were associated with changes in link behavior. However, the rare cases in which packets were received by secondary gateways remain potentially informative, as they may help clarify when multi-gateway reception becomes possible and how it affects the interpretation of link stability and effective range.

V. Conclusion

This study examined the spatial, temporal, and environmental effects on LoRa link characteristics using a one-year deployment of 15 bespoke solar-powered sensors in London. The results show that distance was the dominant control on link quality, with RSSI and SNR generally declining as sensor-to-gateway distance increased. PLR remained consistently low across the deployment, which suggests packet delivery was broadly maintained under weaker signal conditions, although site-specific weak-link behavior was still observed, which motivates a concrete, testable ADR improvement hypothesis of adding PLR and local environment considerations to ADR algorithm. The results also indicate that environmental effects were present but more limited than the distance effect. Higher air temperature was weakly associated with lower ΔRSSI and ΔSNR, whereas no clear relationship was identified between humidity and link quality. Spatially, findings suggest that local land-cover effects are more conditional and may depend on distance, openness, surrounding obstacles, and local activity. Overall, this empirical study contributes to understanding the influence of multiple factors on LoRa signal and LoRaWAN performance in long-term outdoor sensor networks and highlights several constraints that remain relevant for scaling to larger networks for future gateway siting, coverage planning in similar park deployments and for ADR optimization modelling. Future work will integrate longer, larger, more dense deployment to examine whether the observed relationship remains stable over time and whether weaker environmental effects emerge more clearly.

Appendix A

Panoramic photos of deployment site, from sensor 1 -15:

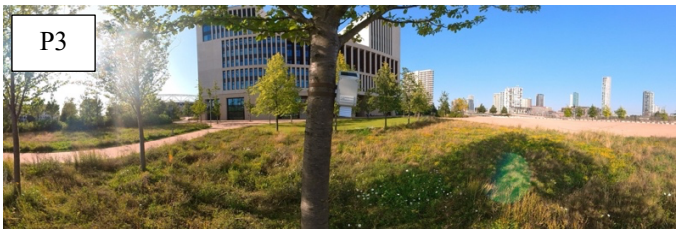

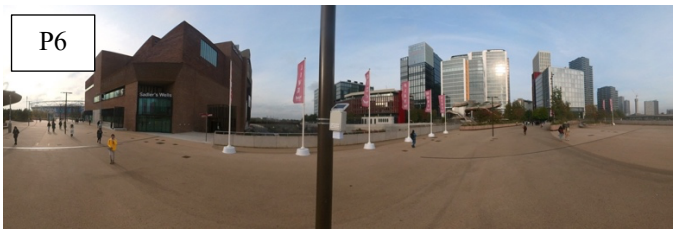

ACKNOWLEDGMENT

We thank the London Legacy Development Corporation for permission to deploy the network in the Queen Elizabeth Olympic Park, and Mr. Simon Gosling for helping with the manufacturing and deployment of the sensors.

REFERENCES

[1] M. Centenaro, L. Vangelista, A. Zanella, and M. Zorzi, 'Long-range communications in unlicensed bands: the rising stars in the IoT and smart city scenarios', *IEEE Wireless Communications*, vol. 23, no. 5, pp. 60–67, Oct. 2016, doi: 10.1109/MWC.2016.7721743.

[2] V. Bonilla, B. Campoverde, and S. G. Yoo, 'A systematic literature review of LoRaWAN: sensors and applications', *Sensors*, vol. 23, no. 20, p. 8440, Jan. 2023, doi: 10.3390/s23208440.

[3] LoRa Alliance, 'LoRaWAN® leads global, at-scale LPWAN deployments across all metrics: most solutions, devices deployed, messages sent and network availability', LoRa Alliance®. Accessed: May 14, 2026. [Online]. Available: https://hz1.37b.myftpupload.com/lora-alliance-press-release/lorawan-leads-global-at-scale-lpwan-deployments-across-all-metrics-most-solutions-devices-deployed-messages-sent-and-network-availability/

[4] J. C. Liando, A. Gamage, A. W. Tengourtius, and M. Li, 'Known and unknown facts of LoRa: experiences from a large-scale measurement study', *ACM Transactions on Sensor Networks*, vol. 15, no. 2, p. 16:1-16:35, Feb. 2019, doi: 10.1145/3293534.

[5] A. E. Ferreira, F. M. Ortiz, L. H. M. K. Costa, B. Foubert, I. Amadou, and N. Mitton, 'A study of the LoRa signal propagation in forest, urban, and suburban environments', *Ann. Telecommun.*, vol. 75, no. 7, pp. 333–351, Aug. 2020, doi: 10.1007/s12243-020-00789-w.

[6] K. Yang, Y. Chen, T. Su, and W. Du, 'Link Quality Modeling for LoRa Networks in Orchards', in *Proceedings of the 22nd International Conference on Information Processing in Sensor Networks*, in IPSN '23. New York, NY, USA: Association for Computing Machinery, May 2023, pp. 27–39. doi: 10.1145/3583120.3586969.

[7] S. Lavdas, G. Vardoulias, W. El Hajj, and Z. Zinonos, 'Performance evaluation of LoRaWAN networks for smart water metering', in *2025 21st International Conference on Distributed Computing in Smart Systems and the Internet of Things (DCOSS-IoT)*, Jun. 2025, pp. 929–935. doi: 10.1109/DCOSS-IoT65416.2025.00141.

[8] S. Lavdas, N. Bakas, K. Vavousis, A. Khalifeh, W. El Hajj, and Z. Zinonos, 'Evaluating LoRaWAN network performance in smart city environments using machine learning', *IEEE Internet of Things Journal*, vol. 12, no. 14, pp. 27060–27074, Jul. 2025, doi: 10.1109/JIOT.2025.3562222.

[9] N. Souza Bezerra, C. Åhlund, S. Saguna, and V. A. de Sousa, 'Temperature impact in LoRaWAN—a case study in northern Sweden', *Sensors*, vol. 19, no. 20, p. 4414, Jan. 2019, doi: 10.3390/s19204414.

[10] T. Ameloot, P. Van Torre, and H. Rogier, 'Variable link performance due to weather effects in a long-range, low-power LoRa sensor network', *Sensors*, vol. 21, no. 9, p. 3128, Jan. 2021, doi: 10.3390/s21093128.

[11] A. Ma, J. T. Rodriguez, M. Sha, and D. Luo, 'Sensorless Air Temperature Sensing Using Lora Link Characteristics', in *2025 21st International Conference on Distributed Computing in Smart Systems and the Internet of Things (DCOSS-IoT)*, Jun. 2025, pp. 1–8. doi: 10.1109/DCOSS-IoT65416.2025.00010.

[12] D. Ma, A. Hudson-Smith, M. De Jode, and L. Lovett, 'Sensing and analysing urban heat islands using internet of things: a real time microclimate network for London', in *Digital-Era Urban Transformations*, R. Goodspeed, E. Suel, H. Chen, J. Barros, and C. Pettit, Eds, Cham: Springer Nature Switzerland, 2025, pp. 247–261. doi: 10.1007/978-3-031-98300-9_14.

[13] D. Ma, A. Hudson-Smith, M. De Jode, and L. Leah, 'Open-source LoRaWAN sensors for distributed IoT networks: crowdsourced environmental data collection for climate resilient cities', in *2025 21st International Conference on Distributed Computing in Smart Systems and the Internet of Things (DCOSS-IoT)*, Jun. 2025, pp. 1–8. doi: 10.1109/DCOSS-IoT65416.2025.00142.

[14] J. Haxhibeqiri, A. Karaagac, F. Van den Abeele, W. Joseph, I. Moerman, and J. Hoebeke, 'LoRa indoor coverage and performance in an industrial environment: Case study', in *2017 22nd IEEE International Conference on Emerging Technologies and Factory Automation (ETFA)*, Sep. 2017, pp. 1–8. doi: 10.1109/ETFA.2017.8247601.